INSTITUT DE FRANCE
Académie des sciences

Comptes Rendus

Chimie

Naima Bayou, Hamid Aït-Amar, Samir Belkhiri, Zohra Bouhila, Fatima Houhoune, Sihem Khemaissia and Tarek Azli

Equilibrium, isotherms and kinetic studies of uranium sorption onto $AlPO_4$-5 and SAPO-5 materials

Volume 24, issue 2 (2021), p. 373-384

Published online: 15 October 2021

https://doi.org/10.5802/crchim.119

Les Comptes Rendus. Chimie *sont membres du*
Centre Mersenne pour l'édition scientifique ouverte
www.centre-mersenne.org
e-ISSN : 1878-1543

Comptes Rendus
Chimie
2021, 24, nº 2, p. 373-384
https://doi.org/10.5802/crchim.119

Full paper / *Article*

Equilibrium, isotherms and kinetic studies of uranium sorption onto $AlPO_4$-5 and SAPO-5 materials

Naima Bayou*, [a], Hamid Aït-Amar [b], Samir Belkhiri [c], Zohra Bouhila [a], Fatima Houhoune [a], Sihem Khemaissia [a] and Tarek Azli [a]

[a] Nuclear Research Center of Draria, (CRND/COMENA), Sebala, Draria PO Box 43, Algiers, Algeria

[b] Laboratory of Engineering Sciences of Industrial Process, University of Sciences and Technology Houari Boumediene, USTHB, BP 32, 16111 El-Alia, Algiers, Algeria

[c] Military Polytechnic School, 16111, Bordj El-Bahri, Algiers, Algeria

E-mails: naima_bayou@yahoo.fr, n-bayou@crnd.dz (N. Bayou), aitamarh@yahoo.com (H. Aït-Amar), samir_belkhiri@yahoo.com (S. Belkhiri), Z-Bouhila@crnd.dz (Z. Bouhila), f-lekouara@crnd.dz (F. Houhoune), S-Khemaissia@crnd.dz (S. Khemaissia), T-Azli@crnd.dz (T. Azli)

Abstract. The present work deals with the investigation of the use of the elaborated aluminophosphate ($AlPO_4$-5) and silico-aluminophosphate (SAPO-5) materials, in uranium sorption from aqueous solution and real effluents obtained from Nuclear Research Center of Draria, Algiers, Algeria. The surface charge and acidic–basic character of $AlPO_4$-5 and SAPO-5 is investigated by the determination of point of zero charge. Batch adsorption experimental studies are carried out to evaluate the influence of initial uranium concentration, final solution pH, contact time, solid-to-liquid ratio and temperature. A maximum adsorption capacity of 61.96 and 74.10 mg/g was obtained for $AlPO_4$-5 and SAPO-5 respectively, at pH 7 with an adsorbent ratio of 0.1/150 g/ml and an equilibrium time of 120 min. Kinetic models (pseudo-first order, pseudo-second order and Weber–Morris) are applied to find the mechanism for the removal of uranium ions, experimental data are analyzed by equilibrium models (Langmuir, Freundlich, Dubinin–Radushkevich and Temkin). Modeling sorption results show that uranium sorption is a chemical and endothermic process. The results showed that $AlPO_4$-5 and SAPO-5 are effective materials for the removal of uranium (VI) ions.

Keywords. Equilibrium, Modeling, Kinetic, Adsorption, Uranium, $AlPO_4$-5, SAPO-5.

Manuscript received 22nd April 2021, revised 7th August 2021, accepted 6th September 2021.

* Corresponding author.

1. Introduction

Environmental pollution due to uranium has largely been as result of development of the nuclear industry [1]. Uranium is the most hazardous long-lived radionuclide in the environment [2]. For both human health security and environment protection, the removal of uranium is necessary [3–5]. Many processes have been used for this purpose such as precipitation, ion exchange, polymeric membrane, solvent extraction, and sorption. Sorption is one of the promising technologies for the removal of toxic heavy metals [6–8]. In this respect, many adsorbents are used such as zeolites and their derivatives [9–16]. Among all these materials, porous zeolite-like aluminophosphate ($AlPO_n$) molecular sieves have the best technological impact due to their catalytic and effective sorptive properties [17]. Synthesis of new materials is made by isomorphic substitution of Al^{3+} and/or P^{5+} by Si (IV), creating a negative charge in the framework of silico-aluminophosphate (SAPO) materials, which considerably influences their sorption capacity [18,19]. The channel diameter of aluminophosphates-five materials (7.3 Å) is larger than the diameter of the hydrated uranyl (6.5 Å) which allowed a possible sorption of uranium by $AlPO_4$-5 and SAPO-5 materials [20,21]. The aim of this work is to improve the sorption of uranium (VI) onto the elaborated $AlPO_4$-5 and SAPO-5, by investigating the experimental sorption parameters such as uranium concentration, pH, solid-to-liquid ratio and temperature. In order to understand the nature of the uranium sorption process, equilibrium and kinetic models are used. Finally, the experimental results are applied to the real effluents from Nuclear Research Center of Draria, Algiers, Algeria.

2. Experiments

2.1. *$AlPO_4$-5 and SAPO-5 elaboration*

According to the literature and our previous work, $AlPO_4$-5 and SAPO-5 are synthesized by hydrothermal crystallization in fluorhydric acid medium [18,22]. The molar gel's composition for SAPO-5 and $AlPO_4$-5 respectively are $0.8Al_2O_3$, $1P_2O_5$, 1.4 R, $0.2SiO_2$, $50H_2O$ and $1Al_2O_3$, $1P_2O_5$, 1.4 R, $50H_2O$, where R is the structuring agent. The gels are introduced into autoclaves and heated at 473 K under autogenic pressure for 24 h. The crystallization is stopped by cooled water. The powders obtained are separated by filtration, washed with distilled water and dried at 353 K overnight. The obtained powders are calcined at 823 K for 6 h.

2.2. *Point of zero charge (PZC) of $AlPO_4$-5 and SAPO-5*

The determination of point of zero charge (PZC) is done to investigate the surface charge and acidic–basic character of $AlPO_4$-5 and SAPO-5 adsorbents. For that KNO_3 (0.01 M) solution is prepared and its initial pH is adjusted between 2 to 11 by adding NaOH (0.1 M) or HNO_3 (0.1 M). Then 10 mL of KNO_3 and 0.1 g adsorbent are interacted in test tubes. The samples are kept at 25 °C for 24 h and the final pH of solutions is measured. The pH_{Pzc} point of $AlPO_4$-5 and SAPO-5 is estimated from the plot of pH_{final}–$pH_{initial}$ versus $pH_{initial}$ of suspensions.

2.3. *Adsorption experiments*

In order to optimize uranyl ion removal conditions, the effect of contact time, initial uranium concentration, pH, solid-to-liquid ratio and temperature are studied. Batch adsorption is performed in polyethylene flasks by agitating a mass m (g) of the adsorbent with a volume V (mL) of solution at different initial concentrations of uranium. The residual concentration of the uranium left in the supernatant phase is determined using a UV-spectrometer following Arsenazo-III method [21,23].

The adsorption uptake and the equilibrium metal uptake capacity q_e (mg/g) are respectively calculated from the following expressions

$$\text{Adsorption uptake} = \frac{C_i - C_{\text{eq}}}{C_i} 100 \tag{1}$$

$$q_e = V \frac{C_i - C_{\text{eq}}}{m} \tag{2}$$

where C_i and C_{eq} are the initial and equilibrium concentrations of uranium ion (mg/L). V is the volume of the solution (L) and m is the mass of adsorbent (g).

2.4. *Error analysis*

The inherent bias resulting from the linearization of the isotherm and kinetic models are highlighted.

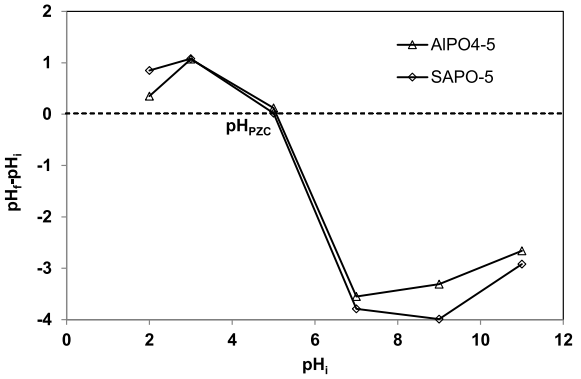

Figure 1. Point of zero charge (PZC) of $AlPO_4$-5 and SAPO-5.

Table 1. Error functions

Error	Function
Root mean square	$\mathrm{RMSE} = \sqrt{\frac{1}{n-2}\sum_{1}^{n}(q_i - q_{ie})^2}$
Chi-squared	$\chi^2 = \sum_{i=1}^{n}\frac{(q_i - q_{ie})^2}{q_{ie}}$
Average relative error	$\mathrm{ARE} = \frac{100}{n}\sum_{i=1}^{n}\left\lvert\frac{q_i - q_{ie}}{q_i}\right\rvert$
Sum of the absolute errors	$\mathrm{SAE} = \sum_{i=1}^{n}\lvert q_i - q_{ie}\rvert_i$

Four different error functions (Table 1), RMSE, χ^2, ARE and SAE, are employed to estimate the fitting quality [23].

The lower values obtained with these error functions favored the isotherm or the kinetic model used in this study.

3. Results and discussion

3.1. *Point of zero charge (PZC)*

The plot of pH_{final}–$pH_{initial}$ versus $pH_{initial}$ for $AlPO_4$-5 and SAPO-5 suspension is shown in the Figure 1. It is interesting to note that the PZC is determined at pH_{final}–$pH_{initial}$ equal to zero and the charge is positive below and negative above the PZC. In the PZC region the pH variation is negligible and lies within ±0.2 pH unit.

The PZC for $AlPO_4$-5 and SAPO-5 used in the present study is found to be 5.00. For pH less than pH_{pzc} = 5 the surface of both materials is generally positively charged and conversely if greater than 5.

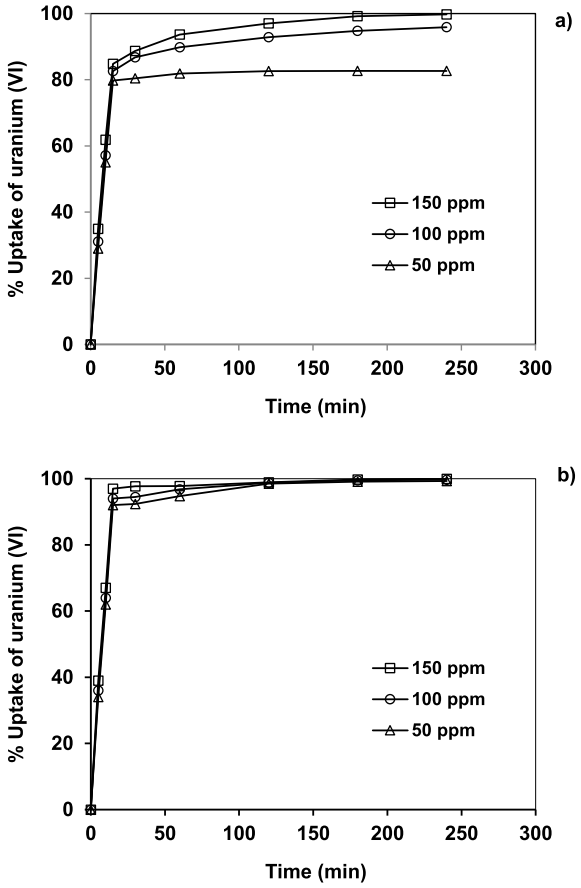

Figure 2. Effect of the initial uranium concentration and contact time on adsorption onto (a) $AlPO_4$-5 and (b) SAPO-5. pH 7, S/L 0.1/150 g/mL, *T* 20 °C.

3.2. *Optimization of the adsorption parameters*

3.2.1. *Effect of the initial uranium concentration and contact time*

Figure 2a and b illustrate the effect of the initial uranium concentration and contact time on the adsorption onto $AlPO_4$-5 and SAPO-5, respectively. Uranium (VI) adsorption uptake for both $AlPO_4$-5 and SAPO-5 increases with initial ion concentration. This is a result of an increase in the driving force, which corresponds to the solution concentration. Also, notice that the amount of uranium ion sorbed increases

rapidly with time in the early stages for both $AlPO_4$-5 and SAPO-5, while the increase is more gradual afterward until equilibrium is reached (120 min). The initial fast sorption could be due to the fact that initially all active sites on the surface of $AlPO_4$-5 and SAPO-5 adsorbents are vacant and the uranium concentration gradient is high. As time elapses the extent of uranium sorption decreases significantly because active sites as well as concentration gradient decreases [24]. The maximum sorption is reached at a contact time of 120 min and the equilibrium values at this time are used in all subsequent measurements.

The uptake of uranium (VI) is larger for SAPO-5 than for $AlPO_4$-5, this behavior may be explained by the silico-aluminophosphate framework negative charge [19,22], which could favor the adsorption of positively charged uranyl ion species UO_2^{2+} through important electrostatic interactions in contrast to the neutral framework of $AlPO_4$-5 [22]. The difference in adsorption capacity of $AlPO_4$-5 and SAPO-5 behavior is also due to the acidity originated by the difference in their constituents. The acidity of $AlPO_4$-5 and SAPO-5 molecular sieves is assigned to both weak Lewis and strong Brönsted acid sites. The weak acidity of $AlPO_4$-5 is related to hydroxyl groups (–OH) bound to the defect sites, i.e. P–OH and Al–OH while weak acidity of SAPO-5 is related to hydroxyl groups (–OH) bound to P–OH, Al–OH and Si–OH (Figure 3) and notice that the bridging hydroxyl groups, i.e. –SiOHAl–, are responsible for the strong acidity of SAPO-5 [25,26].

3.2.2. *Effect of pH*

The pH effect on the removal efficiency of uranium is studied in the range from 2 to 11, using a solution of 50 mg/L of U (VI) at 293 K for 120 min. The influence of the pH on uranium removal is shown in Figure 4.

The results display a strong dependence of uranium (VI) adsorption on solution pH. The uptake of uranium (VI) by adsorption increases with pH up to the value pH = 7, then decreases up to pH = 11. The same trend is observed for both SAPO-5 and $AlPO_4$-5 with a larger percentage U (VI) removal observed for SAPO-5 at all pH values used in this study.

The observed behavior can be explained by the presence of different mononuclear and polynuclear U (VI) hydrolysis products in the form $[(UO_2)_p(OH)_q]^{(2p-q)+}$ at different pH values [27]. At lower pH, there is a high concentration of H^+ ion, which competes with uranyl ion for the binding sites on the surface of sorbent, resulting in a decreased adsorption of uranium (VI) ions. Along with the increase of pH, H^+ ions leave the surface of $AlPO_4$-5 and SAPO-5 making the sites available to the uranium (VI) ions. We can also notice that above PZC = 5, determined in Section 3.1, the SAPO-5 and $AlPO_4$-5 surface charge is negative, favoring the adsorption of positively charged uranyl ions UO_2^{2+}. Moreover, at pH values higher than 7.0, the decrease of adsorption uptake results from the formation of dissolved hydroxide and carbonate complex [28].

3.2.3. *Effect of solid-to-liquid ratio*

Here, we investigate the evolution of the removal uptake of uranium ion onto $AlPO_4$-5 and SAPO-5 aluminophosphate molecular sieves as a function of solid-to-liquid ratio. This effect is highlighted by using 0.1 g of adsorbents mixed with different volumes (10, 30, 40, 100, 150, 200, 250 and 300 mL) of 50 mg/L uranium (VI) solution during 120 min.

The results presented in Figure 5 shows that the uptake of uranium into both adsorbents increase with the solid-to-liquid ratio up to 0.1/150 g/mL. Note that the percentage of uranium uptake is 82 and 98% for $AlPO_4$-5 and SAPO-5 respectively. This is due to the presence of larger adsorption sites on the surface of the adsorbents. Further increase of solid-to-liquid ratio did not increase adsorption much. This behavior can be explained by the saturation of the active sites present in $AlPO_4$-5 and SAPO-5 surfaces by the uranyl ions.

3.2.4. *Effect of Temperature*

The effect of temperature on the adsorption of uranium (VI) is studied by varying the temperature from 293 to 323 K with the other parameters kept constant at their optimum values. The obtained results are reported in Figure 6. It can be observed that the uptake of uranium onto $AlPO_4$-5 and SAPO-5 increases with increasing temperature, indicating that the process is endothermic for both adsorbents used in this study.

3.3. *Adsorption kinetics*

In order to understand the kinetic characteristics of uranium ions adsorption onto $AlPO_4$-5 and SAPO-5

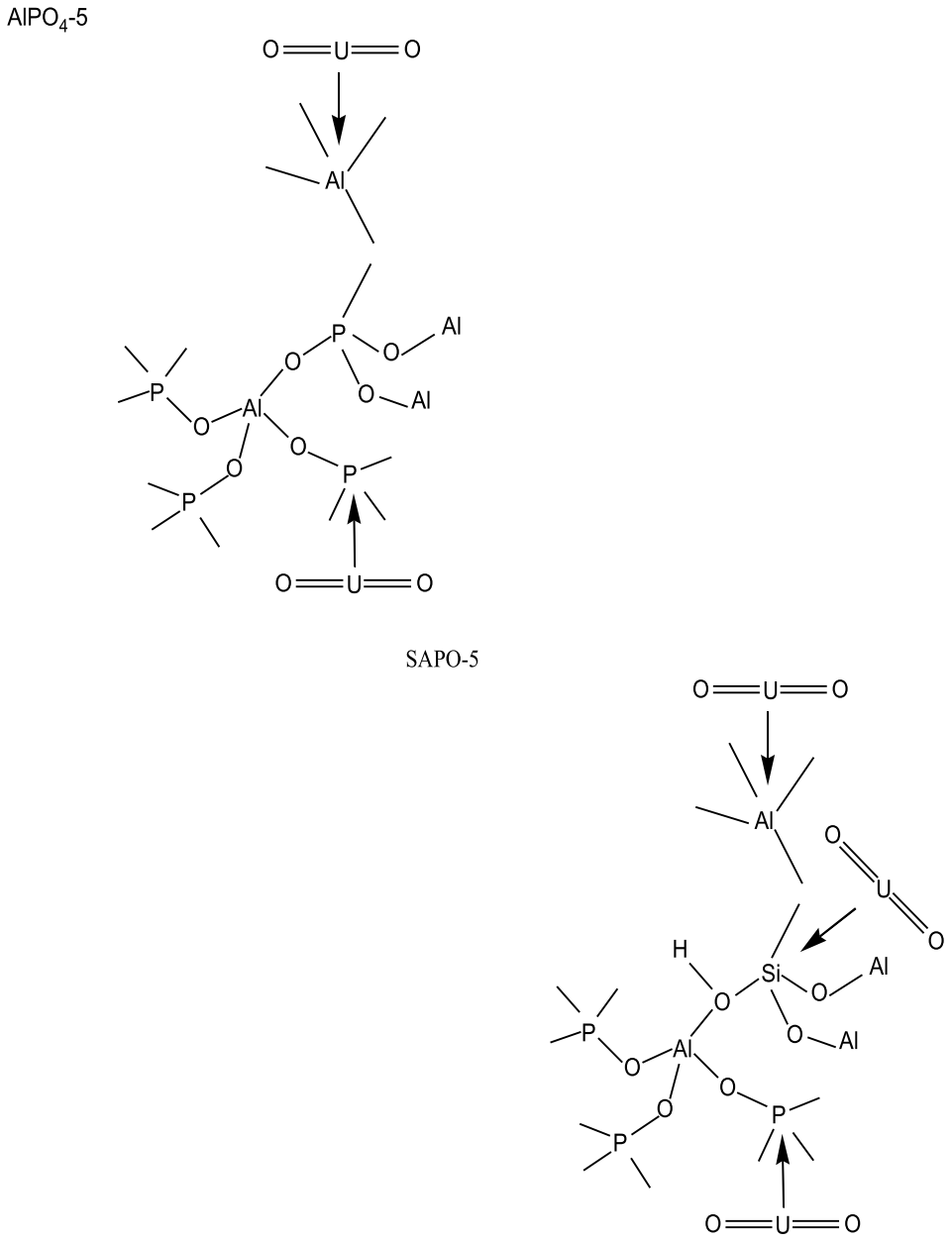

Figure 3. Schematic representation for uranium adsorption onto acidic sites of $AlPO_4$-5 and SAPO-5.

sorbents, three well-known kinetic models namely; pseudo-first order, pseudo-second order and Weber and Morris (Table 2) are tested to evaluate the experimental data for both adsorbents.

The slope and the intercept of the plotting of first order (Figure 7) and second order models (Figure 8) are used to calculate the rate constants and the equilibrium capacities [29], the results are shown in Table 3.

The observed linear regression coefficients close to 1, the calculated values of the adsorption capacity for $AlPO_4$-5 and SAPO-5 close to the experimental values and less error function values reported in Table 3 indicate that the adsorption of uranium (VI) on

Table 2. Kinetic and isotherms models functions and plotting

Isotherm	Functional form	Plotting
Langmuir	$\frac{C_e}{q_e} = \frac{C_e}{q_{\max}} + \frac{1}{bq_{\max}}$	C_e/q_e versus C_e
Freundlich	$\ln q_e = \ln K_f + \frac{1}{n}\ln C_e$	$\ln q_e$ versus $\ln C_e$
Dubinin–Radushkevich	$\ln q_e = \ln q_{\max} - K\varepsilon^2$	$\ln q_e$ versus ε^2
Temkin	$q_e = B_T \ln K_T + B_T \ln C_e$	q_e versus $\ln C_e$
Pseudo-first order	$\log(q_e - q_t) = \log q_e - \frac{k_1 t}{2.303}$	$\log(q_e - q_t)$ versus t
Pseudo-second order	$\frac{t}{q_t} = \frac{t}{q_e} + \frac{1}{h}$ avec $h = k_2 \cdot q_e^2$	t/qt versus t
Weber and Morris	$q_t = k_{id} \cdot t^{0.5} + C$	q_t versus $t^{0.5}$

Table 3. Kinetic parameters of uranium (VI) adsorption by $AlPO_4$-5 and SAPO-5 materials

Kinetic model	Pseudo-first order		Pseudo-second order	
	$AlPO_4$-5	SAPO-5	$AlPO_4$-5	SAPO-5
k_1 (min^{-1})	0.028	0.026	—	—
k_2 (g/mg·min)	—	—	0.098	0.092
q_e (mg/g)	1.37	1.29	53.79	74.07
$q_{e,exp}$ (mg/g)	61.96	74.10	61.96	74.10
R^2	0.82	0.79	0.99	1.00
RMSE	2.40	2.71	0.42	0.42
X^2	26.63	39.96	0.63	0.48
SAE	13.42	15.41	2.44	1.98
ARE	64.93	71.26	1.62	1.28

$AlPO_4$-5 and SAPO-5 fits well the pseudo-second order kinetics. These results suggest that uranium (VI) adsorption appears to be controlled by chemisorption process [30,31].

To identify the diffusion mechanism, the kinetic results are then analyzed by using the intraparticle diffusion model expressed by Weber and Morris equation:

$$q_t = k_{id} \cdot t^{0.5} + C \quad (3)$$

where q_t is the adsorption capacity (mg/g) at time t and k_{id} is the intraparticle diffusion rate constant (mg/g·min). The values of the intercept C provide an indication of the thickness of the boundary layer. If the rate controlling step is intraparticle diffusion, a plot of q_t versus $t^{0.5}$ should yield a straight line passing through the origin. The plot of q_t versus $t^{0.5}$ is shown in Figure 9, where two straight lines with two different slopes are observed for SAPO-5 and $AlPO_4$-5. It is clearly shown that the intraparticle diffusion is not applicable to the entire time scale of the adsorption [32]. The first straight line corresponds to the external surface's fast adsorption. The second straight line is the gradual adsorption stage. A similar two-stage kinetics has been reported earlier [11]. The calculated intraparticle diffusion constants k_{id1} and k_{id2}, C and the obtained correlation coefficients R^2 are presented in Table 4. As expected, the diffusion rate k_{id1} in the first stage is larger than in the second (k_{id2}). Indeed, uranium (VI) is adsorbed

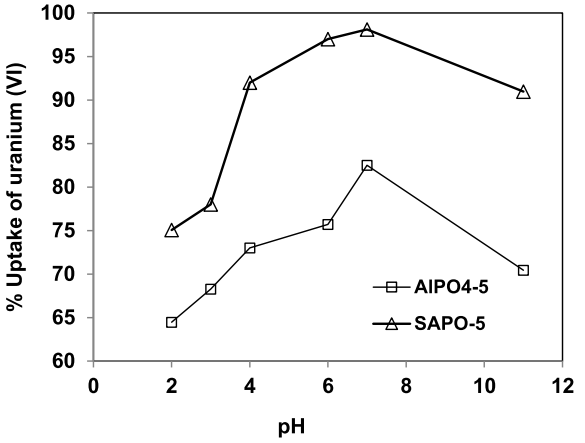

Figure 4. Effect of pH on the uptake percentage of uranium ion onto $AlPO_4$-5 and SAPO-5. *t* 120 min, S/L 0.1/150 g/mL, *T* 20 °C, [U] 50 mg/L.

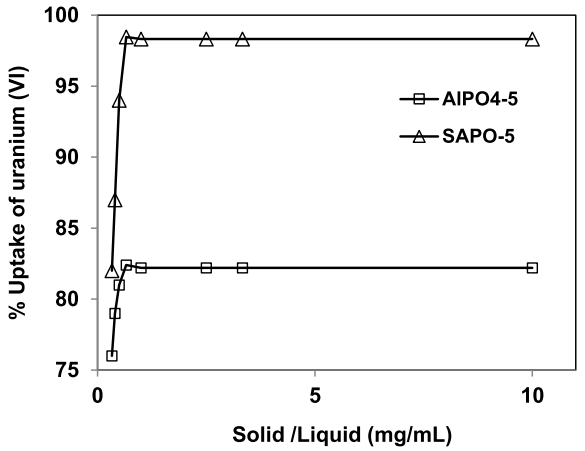

Figure 5. Effect of solid-to-liquid ratio on the removal of U (VI) by $AlPO_4$-5 and SAPO-5. *t* 120 min, *T* 20 °C, pH 7, [U] 50 mg/L.

quickly by the external surface via film diffusion. When the external surface reaches saturation, the uranium (VI) enters the internal pores of the studied materials [3].

The value of the intercept *C* provides information related to the thickness of the boundary layer. Larger values of the intercept obtained for SAPO-5 suggest that the surface diffusion has a larger role as the rate-limiting step [30].

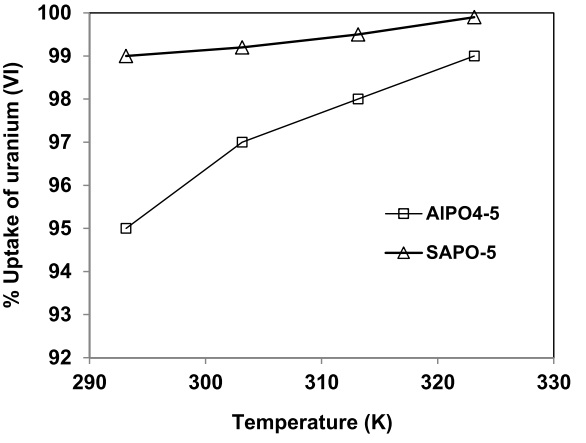

Figure 6. Effect of temperature on the removal of U (VI) by $AlPO_4$-5 and SAPO-5.

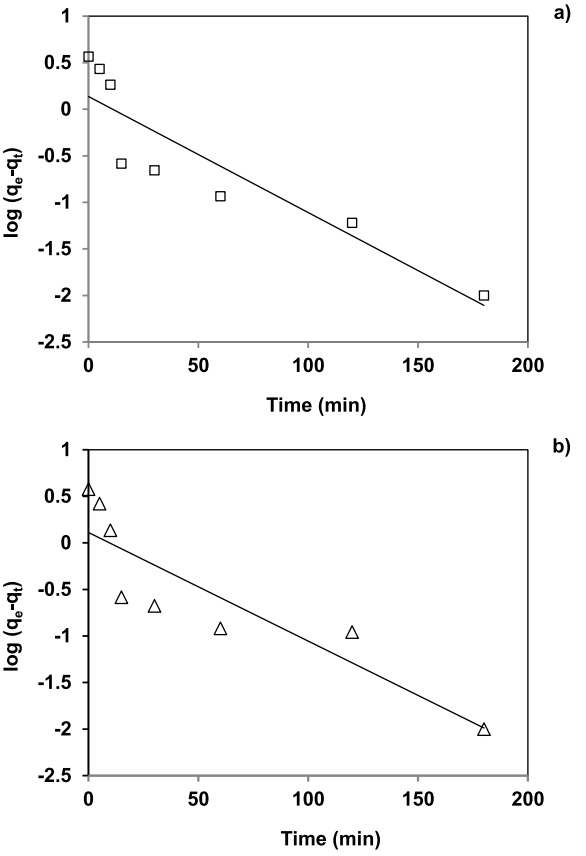

Figure 7. Pseudo-first order plots for the adsorption of uranium (VI) by (a) $AlPO_4$-5 and (b) SAPO-5.

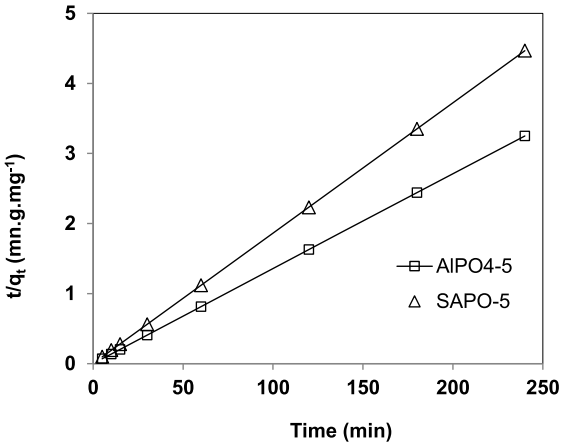

Figure 8. Pseudo-second order plots for the adsorption of uranium (VI) by $AlPO_4$-5 and SAPO-5.

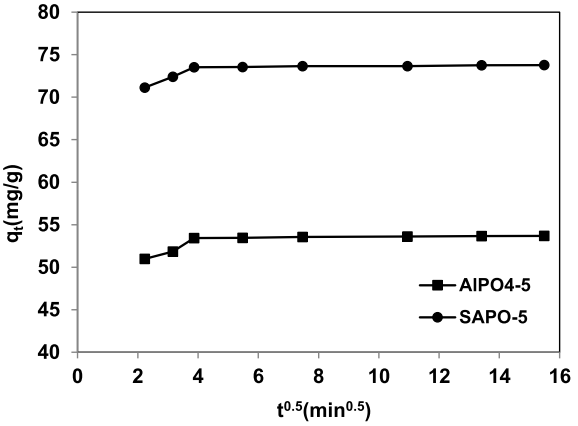

Figure 9. Intraparticle diffusion plots for the uranium adsorption onto $AlPO_4$-5 and SAPO-5.

3.4. *Equilibrium modeling*

The study of equilibrium isotherms is fundamental in supplying the essential information required for the design of a sorption process. Our sorption results are subjected to different sorption isotherms, namely the Langmuir, Freundlich, Dubinin–Radushkevich and Temkin models, which assume a linearized form given in Table 2.

The constants for isotherms, correlation coefficients and error values of Langmuir, Freundlich, D–R and Temkin models are given in Table 5.

Table 4. Intraparticle diffusion rate constants for uranium (VI) adsorption onto $AlPO_4$-5 and SAPO-5 materials

	$AlPO_4$-5	SAPO-5
K_{id1} (mg·g^{-1}·min$^{0.5}$)	1.46	1.44
C_1	47	67
R^2	0.94	0.99
K_{id2} (mg·g^{-1}·min$^{0.5}$)	0.021	0.020
C_2	53	73
R^2	0.92	0.90

The obtained equilibrium values for uranium (VI) uptake with the Langmuir model are 76.92 and 52.63 mg/g for SAPO-5 and $AlPO_4$-5 respectively. These values are close to the experimental adsorption capacity of the adsorbents.

The essential characteristics of the Langmuir isotherm can be explained in terms of a dimensionless constant separation factor R_L defined by:

$$R_L = \frac{1}{1 + bC_i}. \tag{4}$$

The values of R_L indicate the type of isotherm: irreversible ($R_L = 0$), favorable ($0 < R_L < 1$), linear ($R_L = 1$) or unfavorable ($R_L > 1$) [32,33].

The calculated R_L constant values shown in Table 6 lie between 0 and 1 for all uranium concentration values used in this study. This indicates that both $AlPO_4$-5 and SAPO-5 favor uranium (VI) uptake. Similar results have been reported by Jain *et al.* [29], for the removal of Ni(II) from aqueous solution.

The Freundlich model is shown to fit better the SAPO-5 data values with a high correlation coefficient $R^2 = 0.99$ and lower error function values. The Freundlich constant n values should be in the range of 1–10 in order for that adsorption to be favorable [2, 25,32]. The calculated values of n are 1.31 for SAPO-5 and 1.36 for $AlPO_4$-5. These values show the effectiveness of the adsorbents considered in the present study for UO_2^{2+} removal from aqueous solutions.

The analysis of the equilibrium data with the D–R model adsorbents shows a large deviation from linearity for both SAPO-5 and $AlPO_4$-5. This is evidenced by the low R^2 coefficient and the high error function values observed (Table 5). We conclude that the D–R model cannot be applied to the two adsorbents being considered.

Table 5. Model constants and correlation coefficients for adsorption of uranium by aluminophosphate molecular sieves

Model	Langmuir		Freundlich		D–R		Temkin	
	$AlPO_4$-5	SAPO-5	$AlPO_4$-5	SAPO-5	$AlPO_4$-5	SAPO-5	$AlPO_4$-5	SAPO-5
q^{exp} (mg/g)	61.96	74.10						
q_{max} (mg/g)	52.63	76.92						
b (L/g)	0.01	0.04						
K_f (mg/g)			1.14	3.28				
n			1.36	1.31				
q_{max} (mg/g)					20.81	27.54		
$K \cdot 10^6$ (mol^2/kJ^2)					−27.04	−2.61		
K_T							0.17	0.53
B_T							9.84	13.22
$\Delta\theta$ (kJ/mol)							13.03	14.18
R^2	0.97	0.95	0.98	0.99	0.90	0.83	0.99	0.98
RMSE	0.57	0.85	1.39	1.06	10.14	13.76	0.68	4.29
X^2	0.09	0.20	0.47	0.21	24.07	34.38	0.26	4.25
SAE	2.64	4.76	6.52	5.26	47.13	66.34	3.37	19.23
ARE	2.42	4.09	5.40	3.51	77.80	84.47	4.68	15.97

Table 6. R_L values for uranium adsorption obtained from Langmuir equation

$[U]_0$ (mg/L)	40	50	100	150	200
$AlPO_4$-5	0.66	0.61	0.43	0.34	0.28
SAPO-5	0.41	0.36	0.22	0.16	0.12

The experimental data for SAPO-5 and $AlPO_4$-5 are in good agreement with the Temkin model, with a high correlation coefficient and acceptable error functions values.

The obtained positive value of B_T confirms the endothermicity of the process for both adsorbents.

The adsorption energy is useful for predicting whether the adsorption process is physical or chemical in nature.

The adsorption energy $\Delta\theta$ is calculated by using the formula:

$$B_T = q_m \frac{RT}{\Delta\theta}. \quad (5)$$

The $\Delta\theta$ values are 14.18 and 13.03 kJ·mole^{-1} for SAPO-5 and $AlPO_4$-5 respectively, which are greater than 8 kJ·mole^{-1}, indicating that the adsorption process is chemical.

The comparison of the obtained correlation coefficient R^2 and error function values for both $AlPO_4$-5 and SAPO-5 with the selected models shows that the Freundlich model is more appropriate for fitting the uranium (VI) equilibrium data of SAPO-5 while the Temkin model is better for the $AlPO_4$-5 experimental equilibrium data.

3.5. *Behavior of $AlPO_4$-5 and SAPO-5 toward uranium species from real effluent*

The uranium adsorption tests of the synthesized materials are performed using real effluents collected from the Nuclear Research Centre of Draria, Algiers, Algeria.

Experiments for uranium removal from real effluents are performed using the optimized parameters (pH = 7, contact time = 120 min and solid-to-liquid ratio of 0.1/150 (g/mL)). The percentage of adsorption of uranium (VI) ions from real effluents adsorbed onto synthesized $AlPO_4$-5 and SAPO-5 are presented in Figure 10. The percentage of uranium adsorption for $AlPO_4$-5 are important values which are 81.35, 91.57 and 95.98% respectively for

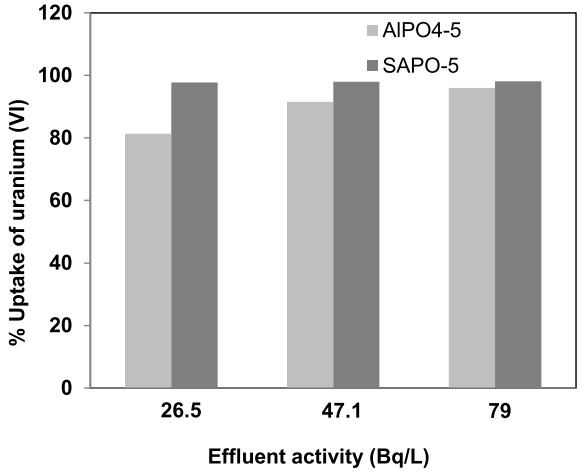

Figure 10. The uranium uptake percentage from real effluents adsorbed onto $AlPO_4$-5 and SAPO-5.

the studied activities of 26.5, 47.1 and 79 Bq/L. Furthermore, SAPO-5 presents larger values with 97.77, 97.98 and 98.11% for the three effluents used in this study.

3.6. *Comparison with other solid adsorbents*

Performance of adsorbents is based on the maximum adsorption capacity of the adsorbent under favorable experimental conditions. Table 7 illustrates the comparison between adsorption capacities of different adsorbents in the removal of uranium [15,33–35].

By comparing these results, both $AlPO_4$-5 and SAPO-5 seem to be very efficient and effective in eliminating uranyl ions, since the adsorption capacity values are important. Comparing the adsorption capacity obtained from synthetic solution and real effluents (Table 7), we can notice a decrease in the adsorption yield in the case of real effluents but still remains important. This behavior may be explained by the presence of the other chemical elements in the effluents [22], which can be co-adsorbed at the same time as the uranium, by occupying the active sites of the adsorbent.

3.7. *Desorption studies*

Desorption study is carried out, after performing adsorption experiments with uranium solution in the concentration of 50, 100 and 150 mg/L, using the two adsorbents $AlPO_4$-5 and SAPO-5. Desorption procedure is carried out using three eluting agents including HCl (0.1 M), H_2SO_4 (0.1 M), and HNO_3 (0.1 M). The desorption experiments are performed by taking 0.1 g of $AlPO_4$-5 and SAPO-5 adsorbent separately, in 50 ml each of eluting solution for 1 h. the uranyl ions desorbed into the eluting solution is separated by centrifugation and analyzed as before.

The desorption ratio is calculated according to the following equation [36]

$$\text{Desorption ratio (\%)} = \frac{\text{Amount of metal ion desorbed}}{\text{Amount of metal ion sorbed}} \times 100. \quad (6)$$

By comparing the results shown in Table 8, it was observed that a higher desorption ratio is obtained when HNO_3 is used for the two adsorbents ($AlPO_4$-5 and SAPO-5). Therefore nitric acid is selected as the best desorbing agent for uranium (VI) ions.

4. Conclusion

In the present study, the elaborated $AlPO_4$-5 and SAPO-5 adsorbents are used in the adsorption of uranium (VI) ion from synthetic and real effluents. The maximum adsorption of uranium (VI) occurs at pH = 7 and solid-to-liquid ratio of 0.1/150 g/mL for both $AlPO_4$-5 and SAPO-5. The equilibrium time is reached within 120 min. Furthermore, SAPO-5 has a negative charge which permits a larger uranium adsorption compared with $AlPO_4$-5. This behavior is due to the presence of silicon on the SAPO-5 framework giving rise to bridging hydroxyl groups, i.e. –Si OHAl, responsible for the strong acidity of SAPO-5.

The observed experimental kinetics data of the studied materials matches with the pseudo-second order model, indicating that the adsorption of uranium (VI) is dominated by chemisorption which is confirmed by modeling results.

Attempts for effective removal of uranium (VI) from real effluents with different activities obtained from Nuclear Research Center of Draria, Algeria using AlPO4-5 and SAPO-5 adsorbents are made. The uptake of uranium ions from real effluents adsorbed onto $AlPO_4$-5 and SAPO-5 is higher than 81% and reached 98%. This study concludes that the elaborated $AlPO_4$-5 and SAPO-5 materials are suitable adsorbent candidates for the removal of uranium.

Table 7. Comparison of the adsorption capacities of $AlPO_4$-5 and SAPO-5 and various adsorbents for uranium (VI)

Adsorbent	Solution	q (mg/g)	Reference
$AlPO_4$-5	Synthetic uranium (VI) solution at 50 mg/L	61.96	This study
	Uranyl effluent at 50 mg/L	61.01	This study
	Synthetic uranium (VI) solution at 100 mg/L	139.26	This study
	Uranyl effluent at 100 mg/L	137.35	This study
	Synthetic uranium (VI) solution at 150 mg/L	218.25	This study
	Uranyl effluent at 150 mg/L	215.95	This study
SAPO-5	Synthetic uranium (VI) solution at 50 mg/L	74.10	This study
	Uranyl effluent at 50 mg/L	73.32	This study
	Synthetic uranium (VI) solution at 100 mg/L	148.78	This study
	Uranyl effluent at 100 mg/L	146.97	This study
	Synthetic uranium (VI) solution at 150 mg/L	223.97	This study
	Uranyl effluent at 150 mg/L	220.74	This study
Carboxylate nanotube		11.73	[33]
4A		100	[34]
Synthetic NaA		6.50	[35]
Synthetic NaY		14.05	[15]

Table 8. The elution of adsorbed uranium ion using different types of eluting agents

Concentration of uranium (mg/L)	% recovery of adsorbed uranium			% recovery of adsorbed uranium		
	SAPO-5			$AlPO_4$-5		
	HCl	H_2SO_4	HNO_3	HCl	H_2SO_4	HNO_3
50	91	89	99	89	87	98
100	90	90	98	87	88	97
150	89	91	99	88	89	98

References

[1] V. M. Efremenkov, "Combined methods for liquid radioactive waste treatment", in *IAEA-TECDOC-1336*, IAEA, Vienna, Austria, 2003, ISSN 10114289.

[2] L. M. Camachoa, S. Denga, R. R. Parra, *J. Hazard. Mater.*, 2010, **175**, 393-398.

[3] M. K. Sureshkumar, D. Das, M. B. Mallia, P. C. Gupta, *J. Hazard. Mater.*, 2010, **184**, 65-72.

[4] R. Han, W. Zou, Y. Wang, L. Zhu, *J. Environ. Radioact.*, 2007, **93**, 127-143.

[5] A. E. Osmanlioglu, *J. Hazard. Mater. B*, 2006, **137**, 332-335.

[6] F. Aydin, M. Soylak, *Talanta*, 2007, **72**, 187-192.

[7] N. Bayou, O. Arous, M. Amara, H. Kerdjoudj, *C. R. Chim.*, 2010, **13**, 1370-1376.

[8] D. James, G. Venkateswaran, T. P. Rao, *Microporous Mesoporous Mater.*, 2009, **119**, 165-170.

[9] R. Donat, *J. Chem. Thermodyn.*, 2009, **41**, 829-835.

[10] P. Ilaiyaraja, A. K. S. Deb, K. Sivasubramanian, D. Ponraju, B. Venkatraman, *J. Hazard. Mater.*, 2013, **250**, 155-166.

[11] R. Akkaya, *J. Environ. Radioact.*, 2013, **120**, 58-63.

[12] A. T. Rodriguez, A. L. Velasco, J. A. Field, R. S. Alvarez, *Water Res.*, 2010, **44**, 2153-2162.

[13] A. Rahmati, A. Ghaemi, M. Samadfam, *Ann. Nucl. Energy*, 2012, **39**, 42-48.

[14] T. S. Anirudhan, S. Rijith, *J. Environ. Radioact.*, 2012, **106**, 8-19.

[15] F. Houhoune, D. Nibou, S. Amokrane, M. Barkat, *Desalin. Water Treat.*, 2013, **5**, 5583-5591.

[16] S. Belkhiri, M. Guerza, S. Chouikh, Y. Boucheffa, Z. Mekhalif, J. Delhalle, C. Colella, *Microporous Mesoporous Mater.*, 2012, **161**, 115-122.

[17] S. T. Wilson, B. M. Lok, E. M. Flanigen, 1982, US Patent 4 310 440.

[18] E. M. Flanigen, *Stud. Surf. Sci. Catal.*, 1988, **37**, 13-27.
[19] J. Kornatowsk, *C. R. Chim.*, 2005, **8**, 561-568.
[20] F. Y. Jiang, Z. K. Tang, J. P. Zhai, J. T. Ye, J. R. Han., *Microporous Mesoporous Mater.*, 2006, **92**, 129-133.
[21] A. Krestou, A. Xenidis, D. Panias, *Miner. Eng.*, 2003, **16**, 1363-1370.
[22] N. Bayou, H. Ait-Amar, M. Attou, S. Menacer, *C. R. Chim.*, 2017, **20**, 704-709.
[23] S. H. Jhung, Y. K. Hwang, J. S. Chang, S. E. Park, *Microporous Mesoporous Mater.*, 2004, **67**, 151-157.
[24] H. Rshakur, K. R. E. Saraee, M. R. Abdi, G. Azimi, *Appl. Radiat. Isot.*, 2016, **118**, 43-55.
[25] A. Izadbakhsh, F. Farhadi, F. Khorasheh, S. Sahebdelfar, M. Asadi, Y. Z. Feng, *Appl. Catal.*, 2009, **364**, 48-56.
[26] D. Arias, A. Colmenares, M. L. Cubeiro, J. Goldwasser, C. M. Lopez, F. J. Machado, V. Sazo, *Catal. Lett.*, 1997, **45**, 51-58.
[27] C. F. Baes, R. E. Mesmer, *The Hydrolysis of Cations*, John Wiley and Sons, New York, 1976.
[28] T. J. Sorg, C. R. Cothern, P. A. Rebers, *J. Environ. Qual.*, 1992, **21**, 151-152.
[29] M. Jain, V. K. Garg, K. Kadirvelu, *Desalin. Water Treat.*, 2014, **52**, 5681-5695.
[30] H. K. Boparai, M. Joseph, D. M. O'Carroll, *J. Hazard. Mater.*, 2011, **186**, 458-465.
[31] L. Tan, Q. Liu, X. Jing, J. Liu, D. Song, S. Hu, L. Liu, J. Wang, *Chem. Eng. J.*, 2015, **2735**, 307-315.
[32] M. Jain, M. Yadav, S. Chaudhry, *Toxine Rev.*, 2020.
[33] M. Rajabi, B. Mirza, K. Mahanpoor, M. Mirjali, F. Najafi, O. Moradi, H. Sadegh, *Ind. Eng. Chem. J.*, 2016, **34**, 130-138.
[34] M. Barkat., D. Nibou, S. Amokrane, s. Chegrouche, A. Mellah, *C. R. Chim.*, 2015, **18**, 261-269.
[35] D. Nibou, S. Khemeissia, S. Amokrane, M. Barkat, S. Chegrouche, A. Mellah, *J. Chem. Eng.*, 2011, **172**, 296-305.
[36] M. Jain, V. K. Garg, U. K. Garg, k. Kadirvelu, M. Sillanpaa, *Int. J. Environ. Res.*, 2015, **9**, 1079-1088.